PAPER

Theoretical insights into the reaction of Cp*(Cl) Hf(diene) with isonitriles†

Ming-Ran Du,‡[a] Xiang-Biao Zhang, ✶[a] Sheng-Meng Si‡[a] and Lei Wang✶[b]

The migratory insertion of isonitriles into a metal–C bond is a potentially important method for C–C bond construction in organic and pharmaceutical syntheses. In this context, the reaction mechanism of Cp*(Cl) Hf(diene) (Cp* = pentamethylcyclopentadienyl) with isonitriles was studied using density functional theory calculations. Hf-imido complexes and α-methylene cyclopentenimines are the confirmed products for N-tert-butyl- or N-1-adamantyl-substituted isonitriles. They are also the thermodynamically favored products of N-2,6-dimethylphenyl (Ar)-substituted isonitriles. The β-H elimination reaction pathway is responsible for the formation of α-methylene cyclopentenimines. Its elementary reactions include the isomerization of Cp*(Cl)Hf(diene), migratory insertion of the first isonitrile into the Hf–C bond, C–C reductive elimination, β-H elimination, migratory insertion of the second isonitrile into the Hf–H bond, C–C reductive coupling, addition of a Hf–H bond, and fragmentation of the six-membered hafnacycle. For methyl-, ethyl-, and Ar-substituted isonitriles, the kinetically favored products are diazahafnacyclopentanes ("σ complexes"). These are formed via an isomerization reaction pathway that comprises isomerization of the Hf complex, C–C reductive coupling, and insertion of a C=N bond. The effects of different substituents on the isonitrile nitrogen on the main elementary reactions are discussed.

Introduction

Hf complexes have attracted considerable attention from chemists owing to their unique reactivities in alkene/olefin polymerization and copolymerization,[1–4] Friedel–Crafts reactions,[5] activation of small molecules such as N_2 and CO_2,[6,7] ring-opening polymerization of cyclic esters,[8] epoxidation,[9] and other important organic reactions.[10–14] Chirik et al. prepared a base-free dihafnocene μ-nitrido complex via CO-induced dinitrogen cleavage. They proved that this complex could serve as a versatile platform to construct N–C bonds via reactions with activated alkynes, organonitriles, CO_2, isocyanates, Me_3SiI, and alkyl triflates.[6] On the other hand, [1,4]-addition of CO to enynes and dienes is very useful in synthesis.[15] As potential replacement of CO, isonitriles could react with radicals, electrophiles, and nucleophiles.[16–22] There are several advantages for using isonitriles over CO. For example, isonitrile reactions do not require high pressures, and the reactivities of isonitriles can be easily modulated by introducing different-

sized electron-donating/withdrawing substituents to the isonitrile nitrogen.

Currently, the migratory insertion of isonitriles into metal–C bonds is becoming a potentially important method for the construction of C–C bonds.[23–26] The resulting iminoacyl and metallaaziridine complexes have also been proven to be versatile intermediates in numerous transition metal-promoted stoichiometric and catalytic transformations. Xie et al. have reported the migratory insertion of isonitriles into Ta–C bonds. They suggested that alkyl and aryl isonitriles exhibit different reactivity patterns, and that the reaction products depend on the type and stoichiometry of these isonitriles.[24a,b] Norton et al. described the migratory insertion of isonitriles into Zr–C bonds. They revealed the reversibility of migratory insertion of tert-butyl (tBu) isonitrile.[24d] The migratory insertion of isonitrile into titanacyclobutane complexes bearing two Cp* (Cp* = pentamethylcyclopentadienyl) moieties provides a pathway for the stereocontrolled synthesis of valuable organic cyclobutanimines.[26f] Recently, Norton et al. reported the reaction of Cp*(Cl)M(2,3-dimethylbutadiene) (M = Ti, **M1a**; M = Hf, **1a**) with isonitriles.[27] The reaction of **M1a** with N-tBu- and N-1-adamantyl (1-Ad)-substituted isonitriles afforded the bis-inserted titanaaziridines at room temperature. Under an elevated temperature and in the presence of pyridine, the titanaaziridine fragments formed the complex cyclic α-methylene cyclopent-3-enimines and Ti imido complexes, while the reaction of **1a** with N-2,6-dimethylphenyl-substituted isonitrile (ArNC) generated a diazahafnacyclopentane with Ar groups

[a]School of Chemical Engineering, Anhui University of Science and Technology, Huainan, Anhui 232001, People's Republic of China. E-mail: xbzhang_theochem@yahoo.com

[b]Department of Chemistry, Huaibei Normal University, Huaibei, Anhui 235000, People's Republic of China. E-mail: leiwang@chnu.edu.cn

‡ These authors contributed equally.

("σ complex"). They pointed out that group 4 metals do mediate the cycloaddition of isonitrile to 2,3-dimethylbutadiene, and the product structure depends upon the nature of the metal. However, the reaction of **1a** with isonitriles in the presence of pyridine has not been investigated. Ballmann *et al.* proved that for the reaction of Hf complexes with isonitriles, the steric effects of different ligands influence the product formation.[28]

In order to expand the application of Hf complexes to C–C bond formation, a comprehensive and unambiguous understanding of the reaction pattern of **1a** with isonitriles is required. In this work, density functional theory (DFT) calculations were performed for the reactions of **1a** with isonitriles bearing *t*Bu, methyl (Me), ethyl (Et), Ar, and 1-Ad groups to answer the following questions: (1) whether α-methylene cyclopentenimines and Hf imido complexes can be produced *via* the reaction of **1a** with isonitriles in the presence of pyridine; (2) if yes, what is the detailed mechanism for their formation; (3) what is the detailed mechanism for the formation of diazahafnacyclopentanes; and (4) the effects of substituent groups on the nitrogen of isonitrile in terms of the reaction mechanisms, and how these substituent groups influence the competition between the afforded products (diazahafnacyclopentanes and α-methylene cyclopentenimines).

Computational details

All calculations were performed using the Gaussian 09 program package.[29] Molecular structures were optimized by the B3LYP/BS1 method.[30,31] Benzene was experimentally adopted as the reaction medium.[27] Thus, benzene solvent effects were taken into account by invoking the polarizable continuum model (PCM) solvation method.[32] In BS1, the Hf and Cl atoms were described by the LANL2DZ basis sets and improved with a set of f- or d-polarization functions ($\alpha = 0.784$ for Hf; $\alpha = 0.640$ for Cl) with effective core potentials (ECP).[33–37] Other atoms were represented by the 6-311+G(d,p) basis sets, except for the atoms on the *t*Bu, Me, Et, Ar, and 1-Ad substituent groups that were described by 6-31G basis sets.[38–40] This theoretical model has proven to be reliable, affording results that were in good agreement with the experimental data [ESI†]. Additionally, frequency calculations were performed to confirm the calculated species as minima (no imaginary frequency) or transition states (only one imaginary frequency), and to provide thermodynamic corrections at 101 325 Pa and 298.15 K. Moreover, intrinsic reaction coordinate (IRC) calculations were carried out to ensure that the afforded transition states were correctly connected to the intended intermediates.[41] Finally, more accurate energies were calculated using the 6-311G(d,p) basis sets instead of the 6-31G basis sets. Corrected Gibbs free energies were used to describe the free-energy profiles of the reaction.

Results and discussion

Mechanism of the reaction of 1a with *t*BuNC

The proposed mechanisms for the reaction of **1a** with *t*BuNC to access α-methylene cyclopentenimine and diazahafnacyclopentane are illustrated in Scheme 1. The reaction pathways in Scheme 1(a)

were calculated first. With a free-energy barrier of 58.6 kJ mol^{-1} [Fig. 1(a)], **1a** isomerizes to **1b** *via* **TS1a-1b**; this reaction is endergonic by 25.1 kJ mol^{-1}. While the 2,3-dimethylbutadiene ligand in **1a** coordinates in a "supine" π-fashion (Fig. 2), the same ligand in **1b** coordinates in a "prone" π-fashion.[42] The two Hf–C(terminal) diene distances (**1a**, Hf–C^1 = 2.25 Å, Hf–C^4 = 2.25 Å; **1b**, Hf–C^1 = 2.24 Å, Hf–C^4 = 2.24 Å) differ from the two Hf–C(internal) diene distances (**1a**, Hf–C^2 = 2.50 Å, Hf–C^3 = 2.50 Å; **1b**, Hf–C^2 = 2.54 Å, Hf–C^3 = 2.54 Å). *t*BuNC coordinates to **1b** with the end-on C atom to afford **2a**. This makes the electronic energy of the system decrease by 21.6 kJ mol^{-1}, and the Gibbs free energy of the system increases by 38.1 kJ mol^{-1} due to the loss of entropy (−171.2 J mol^{-1} K^{-1}). The Hf–C(terminal) diene distances (Hf–C^1 = 2.37 Å, Hf–C^4 = 2.45 Å) in **2a** are longer than those in **1b**. The structure of **2a** maintains the coordinated C=C π-bond, and the two Hf–C(internal) diene distances (Hf–C^2 = 2.45 Å, Hf–C^3 = 2.50 Å) exhibit a stronger interaction between the Hf center and the C=C π-bond than that observed in **1b**. The C=C double bond distance of the butadiene fragment (C^3–C^2 = 1.41 Å) in **2a** is longer than those in **1a** and **1b**. Subsequent migratory insertion of *t*BuNC into the neighboring Hf–C bond requires 35.2 kJ mol^{-1} to furnish **3a** with an uncoordinated N atom, and this is slightly endergonic by 2.1 kJ mol^{-1}. As the C–C σ-bond (C^5–C^4 = 1.92 Å) begins to form in **TS2a-3a**, one Hf–C(terminal) diene distance (Hf–C^4 = 2.60 Å) becomes longer. Moreover, the end-on C atom of *t*BuNC begins to transition from an sp hybridization to an sp^2 state, accompanied by bending of the *t*BuNC moiety. In the "supine" oriented **3a**, the C=C π double bond moiety is repelled out of the Hf center. This is suggested by the Hf–C^2 (2.71 Å) and Hf–C^3 (3.06 Å) distances. Since *t*BuNC directly coordinates to **1a** [Fig. 1(a)] and is subsequently inserted into the Hf–C bond to generate **3d**, the system requires 112.6 kJ mol^{-1} of free energy. This is 14.2 kJ mol^{-1} larger than that required for the favored reaction pathway mentioned above. These results indicate that the isomerization of **1a** to **1b** is indispensable to decrease the free-energy barrier for the insertion to occur. The calculated free-energy barrier for the insertion of *t*BuNC into the Hf–C bond in **2a** is much lower than the 64.5 kJ mol^{-1} required for the migratory insertion of *t*BuNC into the Pd(III)–C bond reported by Yan *et al.*[23c] In turn, the latter is much lower than the 102.1 kJ mol^{-1} required in **2b**. Subsequently, the N atom coordinates to the Hf center to afford **3b**, and this reaction is highly exergonic (58.6 kJ mol^{-1}). The large exergonicity stems from the higher stability of **3b** (having a 14-valence-electron configuration) when compared to that of **3a** (12-valence-electron configuration). The coordination process of the N atom easily takes place and only requires a free-energy barrier <3.8 kJ mol^{-1}. Up to this point, the migratory insertion of the first *t*BuNC is complete and the process is reversible. This is consistent with the reversibility observed for the insertion of *t*BuNC into the Zr–C bond.[24d]

With a free-energy barrier of 33.1 kJ mol^{-1} [Fig. 1(b)], **3b** isomerizes to **3c** *via* **TS3b-3c**. An increase in tension leads to an endergonicity of 25.1 kJ mol^{-1}. C–C reductive elimination from **3c** generates **4** through **TS3c-4**. This process involves Hf–C bond breaking and C–C bond formation, and it needs to overcome a free-energy barrier of 90.4 kJ mol^{-1} and is endergonic by 27.6 kJ mol^{-1}. In **4**, there is a strong agostic interaction between the Hf center and C–H bond. This is indicated by the lengths of
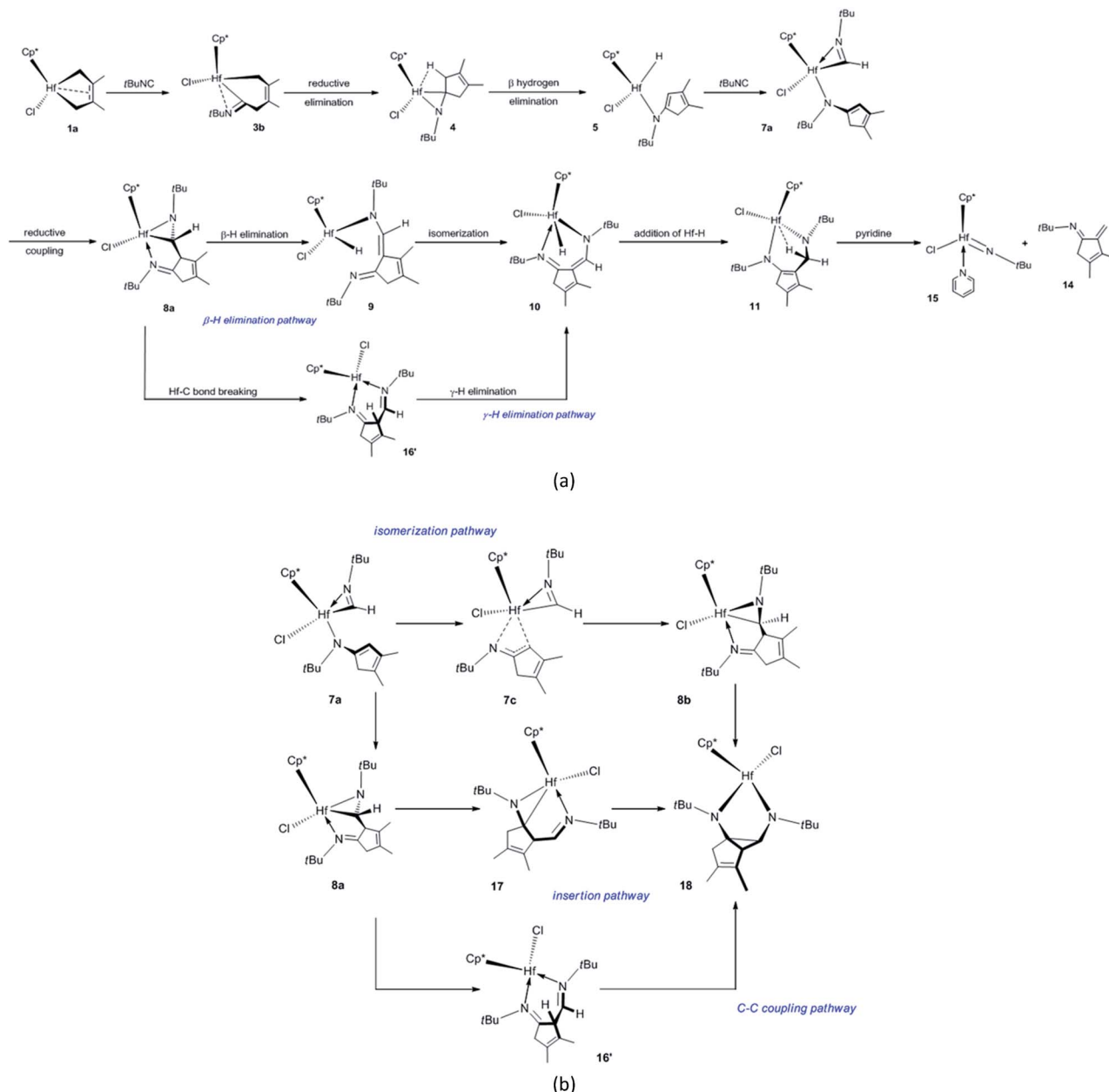
Scheme 1 Proposed mechanisms for (a) the formation of *N-tert*-butyl (*t*Bu)-substituted α-methylene cyclopentenimine and (b) formation of diazahafnacyclopentane **18**.

the Hf–H^1 (2.01 Å) and C^1–H^1 (1.26 Å) bonds. Subsequent β-H elimination rapidly occurs to furnish the Hf hydride **5**. In **5**, the newly formed C=C π double bond conjugates with another of its kind, and the Hf–C bond is completely broken. The conjugation and the release of tension in the three-membered ring make **5** relatively stable, causing the system to be highly exergonic (81.6 kJ mol^{-1}). In **5**, the distance between the Hf center and newly formed π double bond moiety (Hf–C^5 = 2.63 Å, Hf–C^1 = 2.96 Å) indicates that there is almost no interaction between them. The coordination of **5** with the second *t*BuNC generates **6a** with an endergonicity of 43.5 kJ mol^{-1}. The coordination makes the electronic energy and entropy of the system decrease by 4.9 kJ mol^{-1} and 146.9 J mol^{-1} K^{-1}, respectively. Compound

6a satisfies the 14-valence-electron configuration. Subsequently, *t*BuNC is inserted into the Hf–H bond to afford **7a**. The formation of **7a** requires the free-energy barrier of 22.2 kJ mol^{-1} and is exergonic by 78.2 kJ mol^{-1}. **TS6a-7a** belongs to an early transition state where the length of its Hf–H bond is increased by only 0.06 Å. In **7a**, the N atom is coordinated to the Hf center. Compound **7a** is converted to **8a** *via* **TS7a-8a**. This C–C reductive coupling reaction requires a free-energy barrier of 79.9 kJ mol^{-1} and is endergonic by 30.5 kJ mol^{-1}. **TS7a-8a** belongs to a late transition state with a forming C–C bond (1.99 Å) in length.

Clearly, **7a** is the most stable species in the overall *t*BuNC bis-insertion process, its formation requires the free-energy barrier of 122.2 kJ mol^{-1} and is exergonic by 56.9 kJ mol^{-1}, and C–C
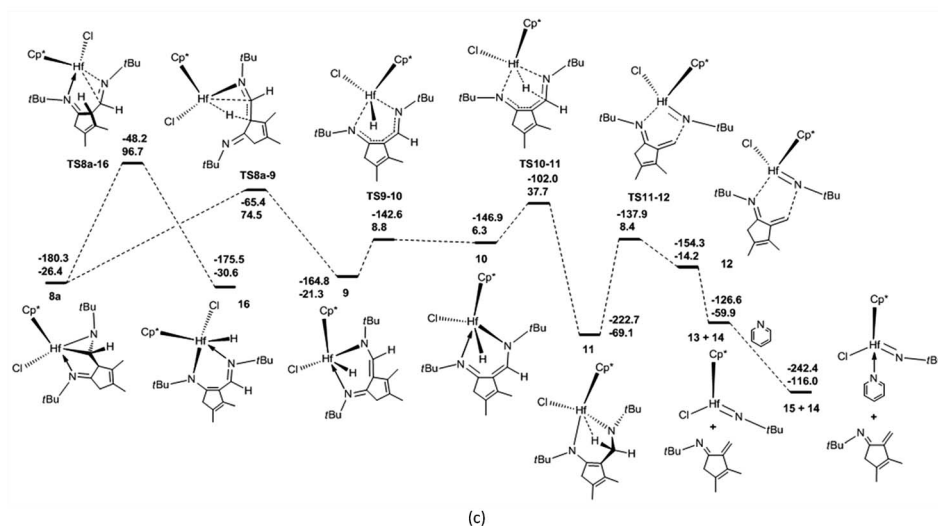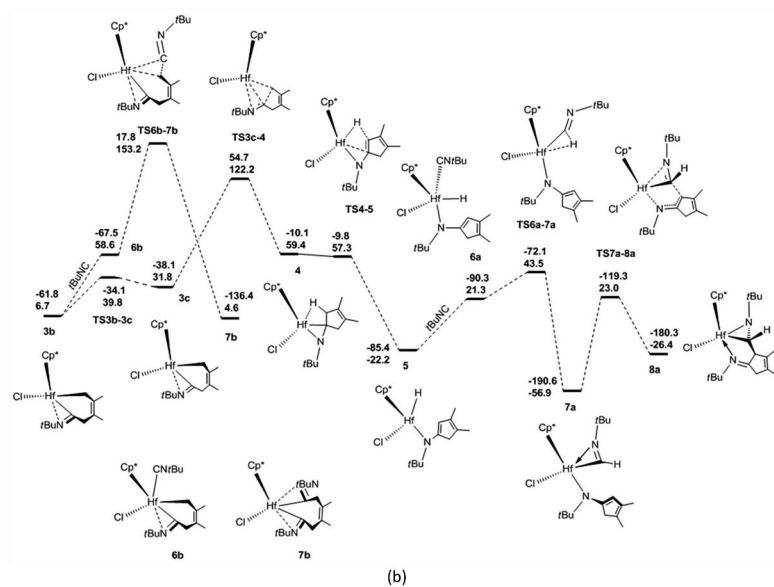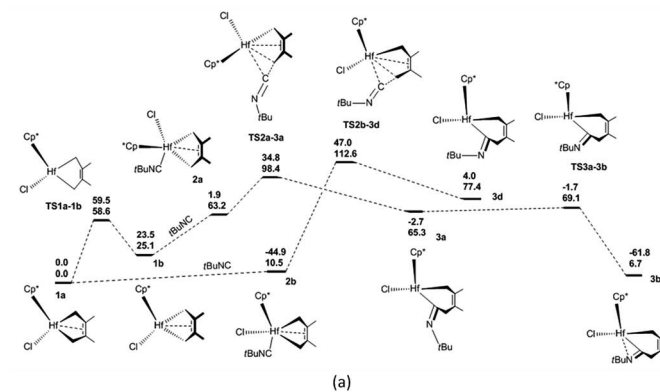
Fig. 1 Free-energy profiles for (a) the insertion of the first *tert*-butyl-substituted isonitrile (*t*BuNC) into Hf−C bond, (b) the insertion of the second *t*BuNC into Hf−H bond as well as into Hf−C bond in **6b**, and (c) the fragmentation of hafnaaziridine **8a**. The electronic energies (above) and Gibbs free energies (below) are given in kJ mol^{-1}.
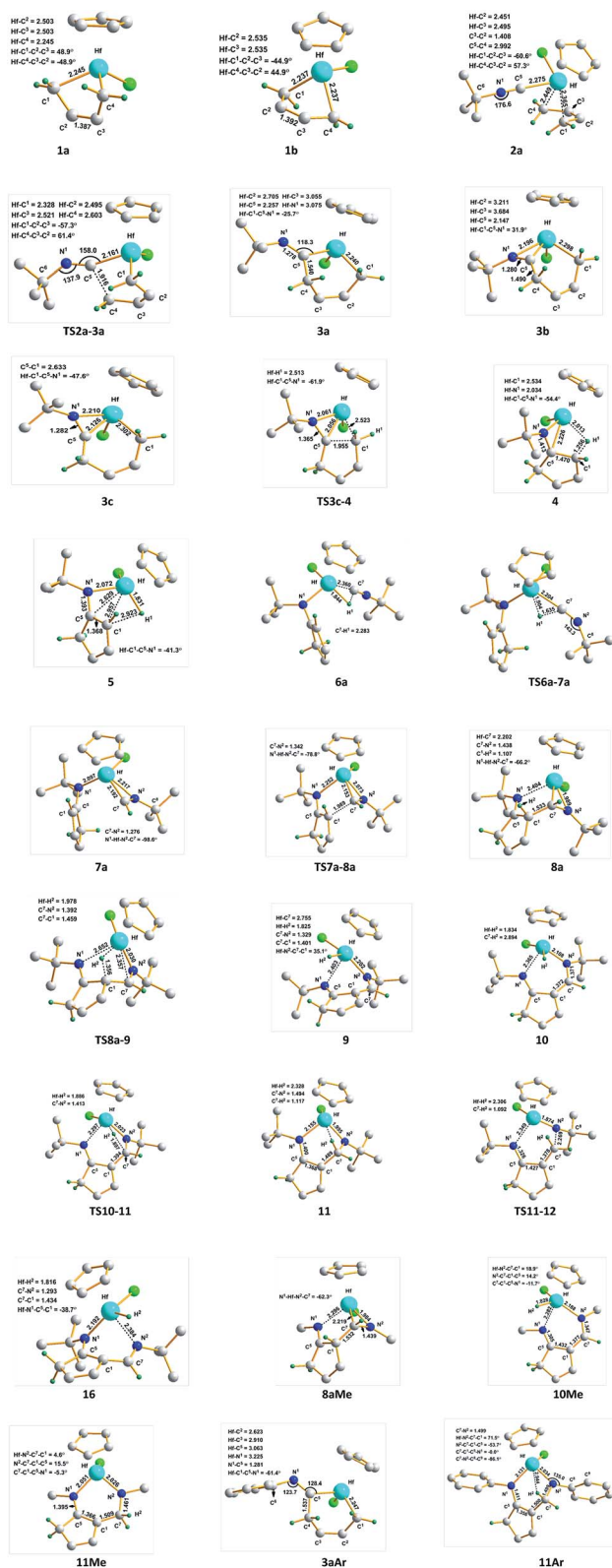
Fig. 2 Optimized structures of selected Hf complexes. The methyl (Me) groups and the H atoms, except for those involved in the reactions, are omitted for clarity. Distances and angles are given in Å and degree, respectively.

reductive elimination is rate-determining. The fused metallabicyclic hafnaaziridine **8a** is an important intermediate. Unfortunately, it cannot be experimentally observed because its formation is thermodynamically unfavorable.

The coordination of *t*BuNC to **3b** [Fig. 1(b)] and the subsequent migratory insertion into the Hf–C bond to generate bis(iminoacyl) hafnacycle **7b** need to overcome a free-energy barrier of 146.5 kJ mol^{-1}; this value is so high that the reaction does not proceed.

Compound **8a** undergoes β-H elimination to afford Hf hydride **9** *via* **TS8a-9** [Fig. 1(c)], the system requires 100.9 kJ mol^{-1} and is endergonic by 5.1 kJ mol^{-1}. In **TS8a-9**, the Hf–H bond is almost formed, and the length of the breaking C–H bond is 0.25 Å longer than that of **8a** (Fig. 2); moreover, the Hf–C bond begins to break. Hf hydride **9** comprises a 14-valence-electron configuration. The ketimine N atoms retain η^1 bonding with the Hf center, while Hf–C is completely broken. Compound **9** overcomes a free-energy barrier (30.1 kJ mol^{-1}) and isomerizes into **10**, the system is endergonic by 27.6 kJ mol^{-1}. The two Hf–N bond lengths in **10** differ by 0.26 Å from each other. With a free-energy barrier of 31.4 kJ mol^{-1}, **10** undergoes the addition of a Hf–H bond across its 1,5-dia-zapentadiene double bond and is converted to the six-membered hafnacycle **11**; the reaction is exergonic by 75.4 kJ mol^{-1}. **TS10-11** is an early transition state with a breaking Hf–H bond slightly longer than that of **10**. Additionally, the length of the C–H bond being formed is 1.90 Å, which is much longer than the usual C–H bond. The length of Hf–H (2.33 Å) in **11** indicates that there is a strong agostic interaction between the Hf center and the newly formed C–H σ-bond. Through **TS11-12**, **11** fragments into Hf imido complex **13** and α-methylene cyclopentenimine **14**. The system requires a free-energy barrier of 77.5 kJ mol^{-1} and is endergonic by 9.2 kJ mol^{-1}. In **TS11-12**, the Hf–N and C–N bonds begin to break, and their lengths are increased by 0.19 Å and 0.78 Å relative to **11**, respectively. The length of Hf–H in **TS11-12** is shortened by 0.02 Å, indicative of a stronger agostic interaction than that observed in **11**. Compound **13** is trapped by pyridine to generate **15** with an exergonicity of 56.1 kJ mol^{-1}.

According to the γ-H elimination reaction pathway [Scheme 1(a)], the calculations show that while the Hf–C bond in **8a** is broken, the H atom spontaneously transfers to the Hf center and **8a** is directly converted to Hf hydride **16** [Fig. 1(c) and 2]; and the hypothesized non-hydride **16'** [Scheme 1(a)] is not obtained. The Hf–C bond requires 123.1 kJ mol^{-1} to break, a value that is larger than the 100.9 kJ mol^{-1} required for β-H elimination from **8a**. Thus, the γ-H elimination reaction pathway is ruled out.

Fig. 1 illustrates that **7a** is a crucial intermediate. The formation of *N*-*t*Bu-substituted α-methylene cyclopentenimine **13** and Hf imido complex **15** requires the free-energy barrier of 131.4 kJ mol^{-1} and is exergonic by 116.0 kJ mol^{-1}, and β-H elimination from **8a** is rate-determining.

There are three proposed reaction mechanisms for the formation of diazahafnacyclopentane **18** [Scheme 1(b)]. (1) In the insertion reaction pathway, **8a** is converted to **17** through the formation and breaking of the Hf–C bonds. Subsequently,

a C=N moiety is inserted into the Hf–C bond in **17** to generate **18**. (2) In the isomerization reaction pathway, **7a** first isomerizes into **7c** that in turn undergoes C–C reductive coupling to afford **8b**. This compound is converted to the target compound **18** *via* the insertion of the C=N moiety into the Hf–C bond. (3) The C–C coupling reaction pathway involves the non-hydride **16′**. However, the above discussion indicates that Hf hydride **16** instead of **16′** is produced after the breaking of the Hf–C bond in **8a**. Thus, this reaction pathway is unfeasible. The calculated free-energy profiles of the insertion and isomerization reaction pathways are shown in Fig. 3. The results show that the isomerization reaction pathway is kinetically more favorable than the insertion one (Fig. 3) but requires high free-energy barrier (146.1 kJ mol⁻¹), and the reaction is endergonic by 39.3 kJ mol⁻¹ [with reference to **7a**; Fig. 3(b)]. This analysis demonstrates that for *t*BuNC, the diazahafnacyclopentane (**18**) formation is kinetically and thermodynamically unfavorable compared to the α-methylene cyclopentenimine (**15**) formation. However, in the experiment of Norton *et al.*, the diazahafnacyclopentane **18** was characterized by NMR spectrum.[27] The inconsistency between the calculation result and experiment could be due to influences of ligands (such as PMe₃), and these influences were not taken into account in our study. In addition, the β-H elimination from **8b** is also unfavorable because the required free energy is too high [146.5 kJ mol⁻¹; Fig. 3(b)].

Effects of substituent groups on the mechanisms and products

In order to reveal the effects of isonitrile *N*-substituent groups on the reaction mechanisms and products, the energetic profiles of the reactions using MeNC, EtNC, ArNC, and 1-AdNC instead of *t*BuNC were calculated (Fig. S1–S5†). The main calculated results are summarized in Scheme 2.

The bis-insertion reaction of MeNC [Scheme 2(a)] reveals a number of differences. (1) The coordination of MeNC to **1b** and hydride **5Me** is endergonic by 35.2 and 20.1 kJ mol⁻¹, respectively, and these values are less than that observed in *t*BuNC. (2) The migratory insertion of MeNC into the Hf–C bond in **2aMe** directly affords the N-coordinated six-membered hafnacycle **3bMe**, overcoming a free-energy barrier of 18.8 kJ mol⁻¹; the reaction is exergonic by 72.4 kJ mol⁻¹. (3) Compared to *t*BuNC, for MeNC the isomerization of the Hf complex **3bMe**, C–C reductive elimination, migratory insertion into the Hf–H bond in **6aMe**, and C–C reductive coupling require less energies (25.5 *vs.* 33.1, 79.2 *vs.* 90.4, 16.7 *vs.* 22.2, and 73.7 *vs.* 79.9 kJ mol⁻¹, respectively). Moreover, the isomerization and reductive coupling reaction steps are less endergonic (15.4 *vs.* 25.1 and 11.7 *vs.* 30.5 kJ mol⁻¹, respectively) while MeNC insertion into the Hf–H bond in **6aMe** is more exergonic (91.3 *vs.* 78.2 kJ mol⁻¹). Additionally, while C–C reductive elimination for *t*BuNC is endergonic, this reaction is exergonic by 16.7 kJ mol⁻¹ in MeNC. These differences are all attributable to the smaller steric effects exhibited by the Me group than that by the *t*Bu group. (4) Finally, β-H elimination from hydride **4Me** requires 47.3 kJ mol⁻¹ to proceed; this is much larger than the value observed for *t*BuNC. This step is exergonic by 45.6 kJ mol⁻¹. Unlike the hydride **4**, there is no strong agostic interaction between the Hf center and the C–H bond in **4Me**, which is responsible for the higher free-energy barrier for the β-H elimination. With a free-energy barrier of 117.7 kJ mol⁻¹ and an exergonicity of 33.0 kJ mol⁻¹, **8aMe** undergoes β-H elimination and is converted to hydride **10Me**. The two Hf–N bond lengths (Hf–N¹ = 2.30 Å and Hf–N² = 1.98 Å) in **8aMe** are shorter than those in **8a**. This indicates that the electron density of the Hf center in the former is higher. Furthermore, the Hf–C bond length (2.22 Å) in **8aMe** is longer than that of **8a** (2.20 Å). These factors led us to determine that the required free-energy barrier for β-H elimination from **8aMe** is larger than that from **8a**. Compared to β-H elimination, the
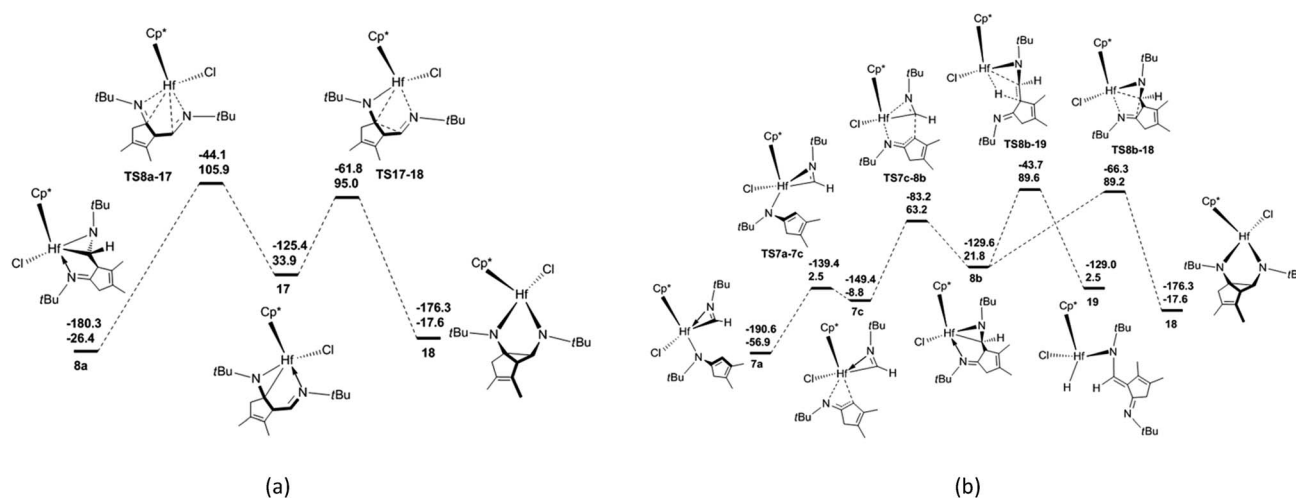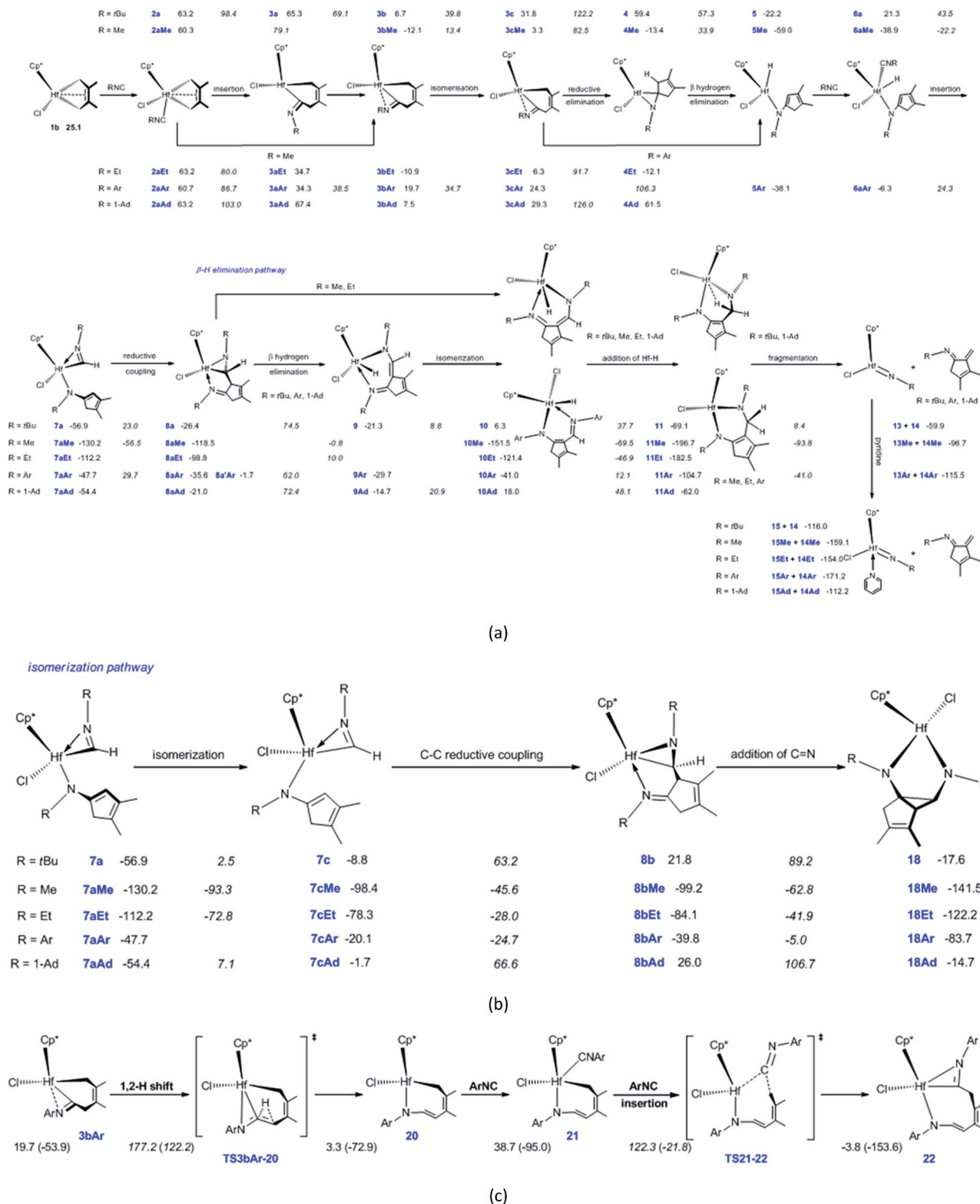

Fig. 3 Free-energy profiles for the formation of diazahafnacyclopentane **18** *via* (a) the insertion reaction pathway and (b) the isomerization reaction pathway and the free-energy profile for β-H elimination from Hf complex **8b**. The electronic energies (above) and Gibbs free energies (below) are given in kJ mol⁻¹.

(a)

(b)

(c)

Scheme 2 Summary of the calculated reaction pathways and results for (a and b) Cp*(Cl)Hf(2,3-dimethylbutadiene) (**1a**) with N-R-substituted isonitriles (values denote Gibbs free energies in kJ mol^{-1} and values in italics are the activation free-energy barriers for elementary reactions), (c) for 1,2-H shift in **3bAr** and ArNC insertion into the Hf–C bond in **21** [the electronic energies (in parentheses) and Gibbs free energies (outside parentheses) are given in kJ mol^{-1}].

breaking of the Hf–C bond in **8aMe** is kinetically unfavorable because it requires 125.6 kJ mol^{-1} to overcome the free-energy barrier. Subsequent addition of a Hf–H bond in **10Me** overcomes the free-energy barrier of 82.0 kJ mol^{-1} to afford the six-membered hafnacycle **11Me**, and this step is exergonic by 45.2 kJ mol^{-1}. Compared to **10**, the configuration of **10Me** does not favor the addition of a Hf–H bond. In **11Me**, there is no agostic interaction between the Hf center and the C–H bond. This is ascribed to the smaller steric effect of the Me group on the nitrogen atom that renders the structure of six-membered hafnacycle **11Me** more planar. With pyridine, the fragmentation of **11Me** to Hf imido complex **15Me** and *N*-Me-substituted α-methylene cyclopentenimine **14Me** is thermodynamically unfavorable, because the system is endergonic by 37.6 kJ mol^{-1}. The six-membered hafnacycle **11Me** requires 129.4 kJ mol^{-1} to form and is exergonic by 196.7 kJ mol^{-1}, thus it is a possible product.

In the formation of diazahafnacyclopentane **18Me**, the isomerization reaction pathway is kinetically more favorable than the insertion reaction pathway (Fig. S2 in ESI†). The isomerization of the Hf complex **7aMe**, C–C reductive coupling, and insertion of C=N into the Hf–C bond in **8bMe** require less energies [36.9 *vs.* 59.4, 52.8 *vs.* 72.0, and 36.4 *vs.* 67.4 kJ mol^{-1}, respectively; Scheme 2(b)] than the corresponding reaction steps for *t*BuNC. Moreover, the C–C reductive coupling is slightly exergonic (0.8 kJ mol^{-1}). This differs from the endergonicity (30.6 kJ mol^{-1}) of the corresponding reaction for *t*BuNC. The insertion of a C=N bond is more exergonic (42.3 kJ mol^{-1}) relative to that of *t*BuNC (39.4 kJ mol^{-1}). For MeNC, the formation of diazahafnacyclopentane **18Me** is kinetically favorable, overcoming a free-energy barrier of 94.6 kJ mol^{-1} and is exergonic by 141.5 kJ mol^{-1}.

Conclusions similar to those for MeNC were reached for the EtNC substrate. The electronic effects of the substituent on the isonitrile nitrogen on some main elementary reactions were examined. Thus, compared to MeNC, (1) the required free-energy barrier for the migratory insertion of EtNC into the Hf–C bond slightly decreases [16.8 *vs.* 18.8 kJ mol^{-1}; Scheme 2(a)]. Moreover, the formed intermediate **3aEt** features an uncoordinated N atom that is related to the relative larger size of the Et moiety. The required free-energy barrier for the C–C reductive elimination increases (85.4 *vs.* 79.2 kJ mol^{-1}). (2) In the β-H elimination reaction pathway, the required energies for β-H elimination and the addition of a Hf–H bond decrease (108.8 *vs.* 117.7 and 74.5 *vs.* 82.0 kJ mol^{-1}, respectively). (3) In the isomerization reaction pathway, isomerization of the Hf complex **7aEt** and insertion of the C=N bond in **8bEt** both overcome higher free-energy barriers [39.4 *vs.* 36.9 and 42.2 *vs.* 36.4 kJ mol^{-1}, respectively; Scheme 2(b)] while C–C reductive coupling in **7cEt** requires a slightly reduced free energy (50.3 *vs.* 52.8 kJ mol^{-1}). These differences are ascribed to the ethyl moiety that renders the Hf center more electron-rich, thus influencing the reactivities of the Hf complexes. According to the shape of the MeNC free-energy profiles (Fig. S2 in ESI†), it can be inferred from Fig. S3 in ESI† that in the case of EtNC, the formation of six-membered hafnacycle **11Et** requires 122.2 kJ mol^{-1} and exhibits an exergonicity of 182.5 kJ mol^{-1}.

Furthermore, the formation of diazahafnacyclopentane **18Et** overcomes a lower free-energy barrier (102.6 kJ mol^{-1}) and is less exergonic (122.2 kJ mol^{-1}).

In the bis-insertion reaction of ArNC, the electron-withdrawing characteristics of the Ar moiety lead to an increase in the free-energy barrier for the insertion of ArNC into the Hf–C bond in **2aAr**, compared to that of EtNC [26.0 *vs.* 16.8 kJ mol^{-1}; Scheme 2(a)]. The formed **3aAr** is a N-uncoordinated six-membered hafnacycle. The isomerization of N-coordinated hafnacycle **3bAr** requires less free-energy (15.0 kJ mol^{-1}) and is less endergonic (4.6 kJ mol^{-1}) compared to the values observed for *t*BuNC and MeNC. These differences are related to the expanded conjugation of the π electrons for ArNC. C–C reductive elimination from **3cAr** overcomes a free-energy barrier of 82.0 kJ mol^{-1} and directly forms Hf hydride **5Ar**, and this step is exergonic by 62.4 kJ mol^{-1}. The required free energy ranges between 90.4 kJ mol^{-1} for *t*BuNC and 79.2 kJ mol^{-1} for MeNC. The insertion of ArNC into the Hf–H bond in **6aAr** overcomes a higher free-energy barrier (30.6 kJ mol^{-1}) and is much less exergonic (41.4 kJ mol^{-1}) compared to that observed for *t*BuNC and MeNC. This is attributed to the more electron-deficient Hf center in the case of ArNC. The required free-energy barrier for C–C reductive coupling in **7aAr** is 3.7 kJ mol^{-1} higher than that of MeNC, and 2.5 kJ mol^{-1} lower than that of *t*BuNC. The shape of the free-energy profile for the pathway leading to α-methylene cyclopentenimine **14Ar** [Fig. S4(b) in ESI†] resembles that of *t*BuNC. However, the electron-withdrawing characteristics of the Ar group lower the free-energy [63.7 kJ mol^{-1}; Scheme 2(a)] required for β-H elimination. Moreover, addition of the Hf–H bond in **10Ar** requires more free energy (53.1 kJ mol^{-1}) for ArNC than for *t*BuNC. Similar to MeNC and EtNC, there is no agostic structure present in the Hf–H bond addition product **11Ar**. Because π-electron delocalization stabilizes the transition state during the fragmentation of **11Ar**, this step requires less free energy (63.7 kJ mol^{-1}) for ArNC than for *t*BuNC and MeNC. In addition, when Ar replaced the *t*Bu group in **TS8a-16**, the afforded **TS(9′-18)Ar** was calculated [Fig. S4(b) in ESI†]. This was proved to be connected to the Hf hydride **9′Ar** and diazahafnacyclopentane **18Ar**; however, the required free energy (156.6 kJ mol^{-1}) is too high. The free-energy profile for the isomerization reaction pathway leading to diazahafnacyclopentane **18Ar** exhibits similar traits to those of MeNC and EtNC. The C–C reductive coupling in **7cAr** and the insertion of C=N in **8bAr** require lower energies [44.8 and 34.8 kJ mol^{-1}, respectively; Scheme 2(b)]. The Ar moiety is an electron-withdrawing but bulkier group. However, its orientation in the Hf complexes can efficiently avoid strong repulsions with other groups. This leads to ArNC reactivities that are similar to those of *t*BuNC as well as MeNC and EtNC. For ArNC, the formation of α-methylene cyclopentenimine **14Ar** and Hf imido complex **15Ar** overcomes a free-energy barrier of 109.7 kJ mol^{-1} and is exergonic by 171.2 kJ mol^{-1} while the formation of diazahafnacyclopentane **18Ar** requires 106.3 kJ mol^{-1} and is exergonic by 83.7 kJ mol^{-1}. Diazahafnacyclopentane **18Ar** has been experimentally produced and characterized by X-ray crystallography.[27] Based on the NMR
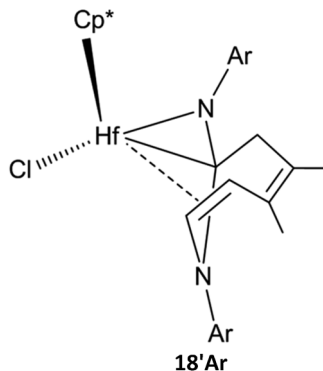
Chart 1

spectrum, Teuben *et al.* proposed that **18′Ar** (see Chart 1) was afforded in the reaction of **1a** with 2ArNC through a 1,2-H shift in **3bAr** followed by the second ArNC insertion into the Hf–C bond.[43] The calculated results show that 1,2-H shift in **3bAr** requires the free-energy barrier of 157.5 kJ mol^{-1} [Scheme 2(c)], and that the apparent activation free energy for the pathway to **18′Ar** as proposed by Teuben *et al.* is not less than 177.2 kJ mol^{-1}. Thus, compared to **18Ar**, the formation of **18′Ar** is kinetically unfavorable.

For 1-AdNC, the calculated reaction free-energy profiles are similar to those of *t*BuNC (Fig. S5 in ESI†). Fig. S5(a)–(c) in ESI† suggest that *N*-1-Ad-substituted α-methylene cyclopentenimine **14Ad** and Hf imido complex **15Ad** can be experimentally afforded: their formation requires 126.8 kJ mol^{-1} and is exergonic by 112.2 kJ mol^{-1}.

Conclusions

The migratory insertion of an isonitrile into a metal–C bond is becoming an increasingly important method for the construction of C–C bonds in organic and pharmaceutical syntheses. In this work, we theoretically studied the reaction of Cp*(Cl)Hf(2,3-dimethylbutadiene) with isonitriles using DFT calculations. Reaction mechanisms for *t*BuNC, MeNC, EtNC, ArNC, and 1-AdNC were proposed and discussed. Unlike the reaction of Cp*(Cl)Ti(2,3-dimethylbutadiene) with isonitriles, the fused three-five metallabicyclic bis-insertion product (hafnaaziridines) predicted in our study could not be experimentally observed, because their formation is thermodynamically unfavorable. For the bulky group (*t*Bu and 1-Ad)-substituted isonitriles, the formation of α-methylene cyclopentenimines and Hf imido complexes was both kinetically and thermodynamically favorable. These reactions exhibited a free-energy barrier of >126 kJ mol^{-1} and were exergonic by ~112 kJ mol^{-1}. For the smaller MeNC and EtNC, the formation of six-membered hafnacycles was thermodynamically more favorable (free-energy barrier of ~122 kJ mol^{-1}; exergonicity >182 kJ mol^{-1}) compared to the formation of the corresponding α-methylene cyclopentenimines and Hf imido complexes. On the other hand, the diazahafnacyclopentanes were the kinetically favored products, with a free-energy barrier of formation <105 kJ mol^{-1}

and exergonicity of <142 kJ mol^{-1}. The Hf imido complex and the α-methylene cyclopentenimine were the thermodynamically favored products for the electron-withdrawing Ar-substituted isonitrile, and the reaction required 109.7 kJ mol^{-1} and was exergonic by 171.2 kJ mol^{-1}. On the other hand, diazahafnacyclopentane was the kinetically favored product with a lower formation free-energy barrier of 106.3 kJ mol^{-1} and an exergonicity of 83.7 kJ mol^{-1}. Moreover, in the formation of α-methylene cyclopentenimines and hafnacycles, the β-H elimination reaction pathway was found to be dominant. This reaction comprises several elementary reaction steps including: the isomerization of Cp*(Cl)Hf(2,3-dimethylbutadiene), migratory insertion of the isonitrile into a Hf–C bond, C–C reductive coupling, migratory insertion of isonitrile into Hf–H bond, β-H elimination, addition of a Hf–H bond, and fragmentation. Finally, an isomerization reaction pathway was found to be responsible for the formation of diazahafnacyclopentanes. This pathway comprises the isomerization of the Hf complex, C–C reductive coupling, and C=N bond insertion as elementary reactions.

Conflicts of interest

There are no conflicts to declare.

Acknowledgements

Notes and references

1 (*a*) G. M. Diamond, K. A. Hall, A. M. LaPointe, M. K. Leclerc, J. Longmire, J. A. W. Shoemaker and P. Sun, *ACS Catal.*, 2011, **1**, 887–900; (*b*) K. Press, V. Venditto, I. Goldberg and M. Kol, *Dalton Trans.*, 2013, **42**, 9096–9103; (*c*) H. Makio, A. V. Prasad, H. Terao, J. Saito and T. Fujita, *Dalton Trans.*, 2013, **42**, 9112–9119; (*d*) I. E. Nifant'ev, P. V. Ivchenko, V. V. Bagrov, S. M. Nagy, L. N. Winslow, J. A. Merrick-Mack, S. Mihan and A. V. Churakov, *Dalton Trans.*, 2013, **42**, 1501–1511.

2 (*a*) L. Rocchigiani, V. Busico, A. Pastore, G. Talarico and A. Macchioni, *Angew. Chem., Int. Ed.*, 2014, **53**, 2157–2161; (*b*) I. Haas, T. Dietel, K. Press, M. Kol and R. Kempe, *Chem.–Eur. J.*, 2013, **19**, 14254–14262; (*c*) S. Mehdiabadi and J. B. P. Soares, *Macromolecules*, 2013, **46**, 1312–1324; (*d*) N. Nakata, T. Toda, T. Matsuo and A. Ishii, *Macromolecules*, 2013, **46**, 6758–6764; (*e*) H. Hamaki, N. Takeda, M. Nabika and N. Tokitoh, *Macromolecules*, 2012, **45**, 1758–1769.

3 (a) X. Wang, Y. Wang, X. Shi, J. Liu, C. Chen and Y. Li, *Macromolecules*, 2014, **47**, 552–559; (b) G. Li, M. Lamberti, G. Roviello and C. Pellecchia, *Organometallics*, 2012, **31**, 6772–6778; (c) E. Szuromi and J. Klosin, *Organometallics*, 2011, **30**, 4589–4597; (d) S. H. Jun, J. H. Park, C. S. Lee, S. Y. Park, M. J. Go, J. Lee and B. Y. Lee, *Organometallics*, 2013, **32**, 7357–7365; (e) P. P. Fontaine, R. Figueroa, S. D. McCann, D. Mort and J. Klosin, *Organometallics*, 2013, **32**, 2963–2972; (f) D. K. Steelman, P. D. Pletcher, J. M. Switzer, S. Xiong, G. A. Medvedev, W. N. Delgass, J. M. Caruthers and M. M. Abu-Omar, *Organometallics*, 2013, **32**, 4862–4867.

4 (a) C. Zhang, H. Pan, J. Klosin, S. Tu and A. Jaganathan, *Org. Process Res. Dev.*, 2015, **19**, 1383–1391; (b) L. He, B. Wang, F. Yang, Y. Li and Z. Ma, *Macromolecules*, 2016, **49**, 6578–6589; (c) Y. Gao, A. R. Mouat, A. Motta, A. Macchioni, C. Zuccaccia, M. Delferro and T. J. Marks, *ACS Catal.*, 2015, **5**, 5272–5282; (d) D. Prema, Y. L. N. M. Arachchige, R. E. Murray and L. M. Slaughter, *Chem. Commun.*, 2015, **51**, 6753–6756; (e) E. Y. Hwang, G. H. Park, C. S. Lee, Y. Young Kang, J. Lee and B. Y. Lee, *Dalton Trans.*, 2015, **44**, 3845–3855.

5 (a) G. Blay, I. Fernández, M. C. Muñoz, J. R. Pedro and C. Vila, *Eur. J. Org. Chem.*, 2013, **2013**, 1902–1907; (b) H. Ishitani, H. Suzuki, Y. Saito, Y. Yamashita and S. Kobayashi, *Eur. J. Org. Chem.*, 2015, **2015**, 5485–5499; (c) Y.-C. Wu, H.-J. Li, L. Liu, N. Demoulin, Z. Liu, D. Wang and Y.-J. Chen, *Adv. Synth. Catal.*, 2011, **353**, 907–912.

6 (a) S. P. Semproni and P. J. Chirik, *J. Am. Chem. Soc.*, 2013, **135**, 11373–11383; (b) S. P. Semproni and P. J. Chirik, *Angew. Chem., Int. Ed.*, 2013, **52**, 12965–12969.

7 (a) F. M. Chadwick, R. T. Cooper and D. O'Hare, *Organometallics*, 2016, **35**, 2092–2100; (b) M. J. Sgro and D. W. Stephan, *Chem. Commun.*, 2013, **49**, 2610–2612.

8 (a) T. K. Saha, V. Ramkumar and D. Chakraborty, *Inorg. Chem.*, 2011, **50**, 2720–2722; (b) S. L. Hancock, M. F. Mahon, G. Kociok-Köhn and M. D. Jones, *Eur. J. Inorg. Chem.*, 2011, **2011**, 4596–4602; (c) L.-C. Liang, S.-T. Lin, C.-C. Chien and M.-T. Chen, *Dalton Trans.*, 2013, **42**, 9286–9293.

9 J. L. Olivares-Romero, Z. Li and H. Yamamoto, *J. Am. Chem. Soc.*, 2012, **134**, 5440–5443.

10 (a) L. Rocchigiani, V. Busico, A. Pastore and A. Macchioni, *Organometallics*, 2016, **35**, 1241–1250; (b) C. Adler, N. Frerichs, M. Schmidtmann and R. Beckhaus, *Organometallics*, 2016, **35**, 3728–3733; (c) M. Kamitani, B. Pinter, C.-H. Chen, M. Pink and D. J. Mindiola, *Angew. Chem., Int. Ed.*, 2014, **53**, 10913–10915; (d) Y. Wang, J. D. Lewis and Y. Román-Leshkov, *ACS Catal.*, 2016, **6**, 2739–2744.

11 (a) R. Waterman and T. D. Tilley, *Chem. Sci.*, 2011, **2**, 1320–1325; (b) T. Beweries, M. Haehnel and U. Rosenthal, *Catal. Sci. Technol.*, 2013, **3**, 18–28; (c) M. de Léséleuc and S. K. Collins, *Chem. Commun.*, 2015, **51**, 10471–10474; (d) M. de Léséleuc and S. K. Collins, *ACS Catal.*, 2015, **5**, 1462–1467; (e) T. De Baerdemaeker, M. Feyen, U. Müller, B. Yilmaz, F.-S. Xiao, W. Zhang, T. Yokoi, X. Bao, H. Gies and D. E. De Vos, *ACS Catal.*, 2015, **5**, 3393–3397.

12 (a) H. Lundberg and H. Adolfsson, *ACS Catal.*, 2015, **5**, 3271–3277; (b) D. L. J. Broere, R. Plessius and J. I. van der Vlugt, *Chem. Soc. Rev.*, 2015, **44**, 6886–6915; (c) Y.-X. Yang, Y. Li, R. Ganguly and C.-W. So, *Dalton Trans.*, 2015, **44**, 12633–12639; (d) H.-J. Chuang, B.-H. Wu, C.-Y. Li and B.-T. Ko, *Eur. J. Inorg. Chem.*, 2014, **2014**, 1239–1248.

13 (a) S. G. Minasian, K. S. Boland, R. K. Feller, A. J. Gaunt, S. A. Kozimor, I. May, S. D. Reilly, B. L. Scott and D. K. Shuh, *Inorg. Chem.*, 2012, **51**, 5728–5736; (b) A. C. Bowman, J. England, S. Sproules, T. Weyhermüller and K. Wieghardt, *Inorg. Chem.*, 2013, **52**, 2242–2256; (c) L.-C. Liang, C.-C. Chien, M.-T. Chen and S.-T. Lin, *Inorg. Chem.*, 2013, **52**, 7709–7716; (d) S. Manabe and Y. J. Ito, *J. Org. Chem.*, 2013, **78**, 4568–4572; (e) T. Gehrmann, G. T. Plundrich, H. Wadepohl and L. H. Gade, *Organometallics*, 2012, **31**, 3346–3354.

14 (a) P. D. Schweizer, H. Wadepohl and L. H. Gade, *Organometallics*, 2014, **33**, 1726–1739; (b) N. Nakata, S. Aoki, V. Y. Lee and A. Sekiguchi, *Organometallics*, 2015, **34**, 2699–2702; (c) P. P. Fontaine, *Organometallics*, 2012, **31**, 6244–6251.

15 (a) S. E. Gibson and A. Stevenazzi, *Angew. Chem., Int. Ed.*, 2003, **42**, 1800–1810; (b) E. J. Corey and S. W. Walinsky, *J. Am. Chem. Soc.*, 1972, **94**, 8932–8933.

16 (a) S. K. Guchhait, V. Chaudhary and C. Madaan, *Org. Biomol. Chem.*, 2012, **10**, 9271–9277; (b) W. Sha, J.-T. Yu, Y. Jiang, H. Yang and J. Cheng, *Chem. Commun.*, 2014, **50**, 9179–9181; (c) Y. Li, A. Chao and F. F. Fleming, *Chem. Commun.*, 2016, **52**, 2111–2113; (d) G. Lesma, I. Bassanini, R. Bortolozzi, C. Colletto, R. Bai, E. Hamel, F. Meneghetti, G. Rainoldi, M. Stucchi, A. Sacchetti, A. Silvani and G. Viola, *Org. Biomol. Chem.*, 2015, **13**, 11633–11644; (e) M. Tobisu and N. Chatani, *Chem. Lett.*, 2011, **40**, 330–340.

17 (a) T. Buyck, D. Pasche, Q. Wang and J. Zhu, *Chem.–Eur. J.*, 2016, **22**, 2278–2281; (b) B. Zhang and A. Studer, *Org. Lett.*, 2014, **16**, 1216–1219; (c) B. Zhang and A. Studer, *Org. Lett.*, 2014, **16**, 3990–3993; (d) Q. Dai, J.-T. Yu, X. Feng, Y. Jiang, H. Yang and J. Cheng, *Adv. Synth. Catal.*, 2014, **356**, 3341–3346.

18 (a) A. Dewanji, C. Mück-Lichtenfeld, K. Bergander, C. G. Daniliuc and A. Studer, *Chem.–Eur. J.*, 2015, **21**, 12295–12298; (b) A. Hinz, A. Schulz and A. Villinger, *J. Am. Chem. Soc.*, 2015, **137**, 9953–9962; (c) N. Shao, G.-X. Pang, C.-X. Yan, G.-F. Shi and Y. Cheng, *J. Org. Chem.*, 2011, **76**, 7458–7465; (d) S. U. Dighe, A. K. K. S., S. Srivastava, P. Shukla, S. Singh, M. Dikshit and S. Batra, *J. Org. Chem.*, 2015, **80**, 99–108.

19 (a) Y. Li and F. F. Fleming, *Angew. Chem., Int. Ed.*, 2016, **55**, 14770–14773; (b) D. Riedel, T. Wurm, K. Graf, M. Rudolph, F. Rominger and A. S. K. Hashmi, *Adv. Synth. Catal.*, 2015, **357**, 1515–1523; (c) M. Seidl, M. Schiffer, M. Bodensteiner, A. Y. Timoshkin and M. Scheer, *Chem.–Eur. J.*, 2013, **19**, 13787–13791; (d) S. Tong, Q. Wang, M.-X. Wang and J. Zhu, *Angew. Chem., Int. Ed.*, 2015, **54**, 1293–1297.

20 (a) S. Tong, Q. Wang, M.-X. Wang and J. Zhu, *Chem.–Eur. J.*, 2016, **22**, 8332–8338; (b) R. M. Wilson, J. L. Stockdill, X. Wu, X. Li, P. A. Vadola, P. K. Park, P. Wang and S. J. Danishefsky, *Angew. Chem., Int. Ed.*, 2012, **51**, 2834–2848; (c) B. Zhang, C. Mück-Lichtenfeld, C. G. Daniliuc and A. Studer, *Angew. Chem., Int. Ed.*, 2013, **52**, 10792–10795; (d) A. S. K. Hashmi, C. Lothschütz, C. Böhling and F. Rominger, *Organometallics*, 2011, **30**, 2411–2417.

21 (a) H. Zhang, D. Shi, S. Ren, H. Jin and Y. Liu, *Eur. J. Org. Chem.*, 2016, **2016**, 4224–4229; (b) R. S. Chay, K. V. Luzyanin, V. Y. Kukushkin, M. F. C. Guedes da Silva and A. J. L. Pombeiro, *Organometallics*, 2012, **31**, 2379–2387; (c) H. V. Le and B. Ganem, *Org. Lett.*, 2011, **13**, 2584; (d) M. Maj, C. Ahn, D. Kossowska, K. Park, K. Kwak, H. Han and M. Cho, *Phys. Chem. Chem. Phys.*, 2015, **17**, 11770–11778.

22 (a) M. Adib, S. Feizi, M. S. Shirazi, L.-G. Zhu and H. R. Bijanzadeh, *Helv. Chim. Acta*, 2014, **97**, 524–531; (b) H. Stöckmann, A. A. Neves, S. Stairs, K. M. Brindle and F. J. Leeper, *Org. Biomol. Chem.*, 2011, **9**, 7303–7305; (c) G. Bianchini, G. L. Sorella, N. Canever, A. Scarso and G. Strukul, *Chem. Commun.*, 2013, **49**, 5322–5324.

23 (a) A. Zeiler, M. Rudolph, F. Rominger and A. S. K. Hashmi, *Chem.–Eur. J.*, 2015, **21**, 11065–11071; (b) G. Pendecy and S. Batra, *RSC Adv.*, 2015, **5**, 28875–28878; (c) H. Gu, Z. Qiu, Z. Zhang, J. Li and B. Yan, *Dalton Trans.*, 2015, **44**, 9839–9846; (d) H. Jiang, H. Gao, B. Liu and W. Wu, *Chem. Commun.*, 2014, **50**, 15348–15351.

24 (a) L. Xiang and Z. Xie, *Organometallics*, 2016, **35**, 233–241; (b) L. Xiang and Z. Xie, *Organometallics*, 2016, **35**, 1430–1439; (c) K. Takamatsu, K. Hirano and M. Miura, *Org. Lett.*, 2015, **17**, 4066–4069; (d) T. N. Valadez, J. R. Norton, M. C. Neary and P. J. Quinlivan, *Organometallics*, 2016, **35**, 3163–3169.

25 (a) F. Foschi, T. Roth, H. Wadepohl and L. H. Gade, *Org. Lett.*, 2016, **18**, 5182–5185; (b) H. Braunschweig, M. A. Celik, R. D. Dewhurst, K. Ferkinghoff, A. Hermann, J. O. C. Jimenez-Halla, T. Kramer, K. Radacki, R. Shang, E. Siedler, F. Weißenberger and C. Werner, *Chem.–Eur. J.*, 2016, **22**, 11736–11744; (c) C.-H. Lei, D.-X. Wang, L. Zhao, J. Zhu and M.-X. Wang, *J. Am. Chem. Soc.*, 2013, **135**, 4708–4711; (d) W. Lu, H. Lu, Y. Li, R. Ganguly and R. Kinjo, *J. Am. Chem. Soc.*, 2016, **138**, 6650–6661.

26 (a) H.-Y. Tu, Y.-R. Liu, J.-J. Chu, B.-L. Hu and X.-G. Zhang, *J. Org. Chem.*, 2014, **79**, 9907–9912; (b) M. Ma, A. Stasch and C. Jones, *Chem.–Eur. J.*, 2012, **18**, 10669–10676; (c) Y. Odabachian, S. Tong, Q. Wang, M.-X. Wang and J. Zhu, *Angew. Chem., Int. Ed.*, 2013, **52**, 10878–10882; (d) A. G. Tskhovrebov, K. V. Luzyanin, F. M. Dolgushin, M. F. C. Guedes da Silva, A. J. L. Pombeiro and V. Y. Kukushkin, *Organometallics*, 2011, **30**, 3362–3370; (e) M. Okazaki, K. Suto, N. Kudo, M. Takano and F. Ozawa, *Organometallics*, 2012, **31**, 4110–4113; (f) G. Greidanus-Strom, C. A. G. Carter and J. M. Stryker, *Organometallics*, 2002, **21**, 1011–1013.

27 T. N. Valadez, J. R. Norton and M. C. Neary, *J. Am. Chem. Soc.*, 2015, **137**, 10152–10155.

28 S. Batke, M. Sietzen, L. Merz, H. Wadepohl and J. Ballmann, *Organometallics*, 2016, **35**, 2294–2308.

29 M. J. Frisch, G. W. Trucks, H. B. Schlegel, G. E. Scuseria, M. A. Robb, J. R. Cheeseman, G. Scalmani, V. Barone, B. Mennucci, G. A. Petersson, H. Nakatsuji, M. Caricato, X. Li, H. P. Hratchian, A. F. Izmaylov, J. Bloino, G. Zheng, J. L. Sonnenberg, M. Hada, M. Ehara, K. Toyota, R. Fukuda, J. Hasegawa, M. Ishida, T. Nakajima, Y. Honda, O. Kitao, H. Nakai, T. Vreven, J. A. Montgomery, J. E. Peralta, F. Ogliaro, M. Bearpark, J. J. Heyd, E. Brothers, K. N. Kudin, V. N. Staroverov, R. Kobayashi, J. Normand, K. Raghavachari, A. Rendell, J. C. Burant, S. S. Iyengar, J. Tomasi, M. Cossi, N. Rega, J. M. Millam, M. Klene, J. E. Knox, J. B. Cross, V. Bakken, C. Adamo, J. Jaramillo, R. Gomperts, R. E. Stratmann, O. Yazyev, A. J. Austin, R. Cammi, C. Pomelli, J. W. Ochterski, R. L. Martin, K. Morokuma, V. G. Zakrzewski, G. A. Voth, P. Salvador, J. J. Dannenberg, S. Dapprich, A. D. Daniels, O. Farkas, J. B. Foresman, J. V. Ortiz, J. Cioslowski and D. J. Fox, *Gaussian 09, revision A.02*, Gaussian, Inc., Wallingford, CT, 2009.

30 A. D. Becke, *J. Chem. Phys.*, 1993, **98**, 5648–5652.

31 C. Lee, W. Yang and R. G. Parr, *Phys. Rev. B: Condens. Matter Mater. Phys.*, 1988, **37**, 785–789.

32 J. Tomasi, B. Mennucci and R. Cammi, *Chem. Rev.*, 2005, **105**, 2999–3094.

33 P. J. Hay and W. R. Wadt, *J. Chem. Phys.*, 1985, **82**, 270–283.

34 W. R. Wadt and P. J. Hay, *J. Chem. Phys.*, 1985, **82**, 284–298.

35 A. W. Ehlers, M. Böhme, S. Dapprich, A. Gobbi, A. Höllwarth, V. Jonas, K. F. Köhler, R. Stegmann, A. Veldkamp and G. Frenking, *Chem. Phys. Lett.*, 1993, **208**, 111–114.

36 A. Höllwarth, M. Böhme, S. Dapprich, A. W. Ehlers, A. Gobbi, V. Jonas, K. F. Köhler, R. Stegmann, A. Veldkamp and G. Frenking, *Chem. Phys. Lett.*, 1993, **208**, 237–240.

37 P. J. Hay and W. R. Wadt, *J. Chem. Phys.*, 1985, **82**, 299–310.

38 W. J. Hehre, R. Ditchfield and J. A. Pople, *J. Chem. Phys.*, 1972, **56**, 2257–2261.

39 R. Krishnan, J. S. Binkley, R. Seeger and J. A. Pople, *J. Chem. Phys.*, 1972, **72**, 650–654.

40 V. A. Rassolov, M. A. Ratner, J. A. Pople, P. C. Redfern and L. A. Curtiss, *J. Comput. Chem.*, 2001, **22**, 976–984.

41 (a) C. Gonzalez and H. B. Schlegel, *J. Chem. Phys.*, 1989, **90**, 2154–2161; (b) C. Gonzalez and H. B. Schlegel, *J. Phys. Chem.*, 1990, **94**, 5523–5527.

42 D. D. Devore, F. J. Timmers and D. L. Hasha, *Organometallics*, 1995, **14**, 3132–3134.

43 B. Hessen, H. Blenkers and J. H. Teuben, *Organometallics*, 1989, **8**, 830–835.